Fusion Engineering and Design 119 (2017) 22–28

Contents lists available at ScienceDirect

Fusion Engineering and Design

journal homepage: www.elsevier.com/locate/fusengdes

Options for a high heat flux enabled helium cooled first wall for DEMO

Frederik Arbeiter*, Yuming Chen, Bradut-Eugen Ghidersa, Christine Klein, Heiko Neuberger, Sebastian Ruck, Georg Schlindwein, Florian Schwab, Axel von der Weth

Karlsruhe Institute of Technology, Institute of Neutron Physics and Reactor Technology, Hermann-von-Helmholtz-Platz 1, 76344 Eggenstein-Leopoldshafen, Germany

HIGHLIGHTS

- Design challenges for helium cooled first wall reviewed and otimization approaches explored.
- Application of enhanced heat transfer surfaces to the First Wall cooling channels.
- Demonstrated a design point for 1 MW/m^2 with temperatures <550 °C and acceptable stresses.
- Feasibility of several manufacturing processes for ribbed surfaces is shown.

ARTICLE INFO

Article history:
Received 28 October 2016
Received in revised form 13 April 2017
Accepted 21 April 2017
Available online 4 May 2017

Keywords:
Plasma Facing Components
First Wall
Helium
Thermo-mechanics
Heat transfer enhancement
Design optimization

ABSTRACT

Helium is considered as coolant in the plasma facing first wall of several blanket concepts for DEMO fusion reactors, due to the favorable properties of flexible temperature range, chemical inertness, no activation, comparatively low effort to remove tritium from the gas and no chemical corrosion. Existing blanket designs have shown the ability to use helium cooled first walls with heat flux densities of 0.5 MW/m^2. Average steady state heat loads coming from the plasma for current EU DEMO concepts are expected in the range of 0.3 MW/m^2. The definition of peak values is still ongoing and depends on the chosen first wall shape, magnetic configuration and assumptions on the fraction of radiated power and power fall off lengths in the scrape off layer of the plasma. Peak steady state values could reach and excess 1 MW/m^2. Higher short-term transient loads are expected.

Design optimization approaches including heat transfer enhancement, local heat transfer tuning and shape optimization of the channel cross section are discussed. Design points to enable a helium cooled first wall capable to sustain heat flux densities of 1 MW/m^2 at an average shell temperature lower than 500 °C are developed based on experimentally validated heat transfer coefficients of structured channel surfaces. The required pumping power is in the range of 3–5% of the collected thermal power. The FEM stress analyses show code-acceptable stress intensities. Several manufacturing methods enabling the application of the suggested heat transfer enhanced first wall channels are explored. An alternative cooling technology is suggested, extending the tolerable heat loads up to 3 MW/m^2.

1. Introduction

The use of high pressure helium gas as coolant medium for the First Wall (FW) is foreseen for several blanket concepts (Helium Cooled Pebble Bed (HCPB), Helium Cooled Lithium Lead (HCLL), Dual Coolant Lithium Lead (DCLL)) for the EU DEMO [1] and has already been developed to sustain moderate heat flux densities in the range of 250–500 kW/m^2, supported by analyses [2–4] and experiments [4]. The main advantages of helium as coolant are: (1) the flexibility to match the structural material's upper and lower temperature limits, (2) safety aspects such as chemical inertness (avoid reactions with neutron multiplier or breeder materials), no activation, comparatively low effort to remove tritium from the gas, and (3) no chemical corrosion. Among the challenges for helium as coolant medium are the lower product of density and heat capacity and lower thermal conductivity. This leads (1) to larger required pumping power for the same cooling as well as (2) to usually wider cooling channel cross sections, which give rise to bending stresses

* Corresponding author.
E-mail address: f.arbe@kit.edu (F. Arbeiter).

http://dx.doi.org/10.1016/j.fusengdes.2017.04.083

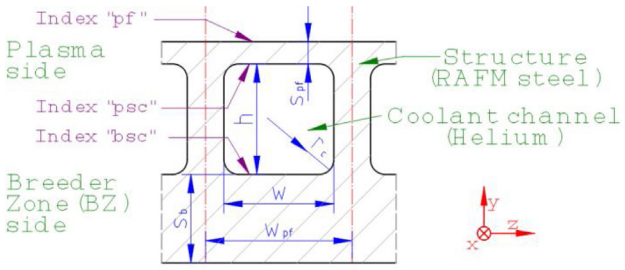

Fig. 1. Naming convention for orientation and measures of a FW channel element (cross section shown).

in the plasma sided channel cover. This paper proposes measures to deal with the above-mentioned challenges.

2. FW thermal-mechanical loads

Several studies were published recently on the expected FW thermal loads in the EU DEMO. Radiated power was estimated up to 450 kW/m^2 [5], and additional peak loads by thermal charged particles were estimated up to 650 kW/m^2 [6] or even in the several MW/m^2 region for cases where the FW surfaces intersect with the magnetic field lines (which is the case for some suggested FW contours) [7]. Peaking of the heat flux density vs. the average value makes the FW/blanket cooling design complicated and the balance-of-plant less efficient, because the ratio of harvested thermal power vs. the pumping power ($\dot{Q}_{th}/P_{pump}$) drops progressively for higher heat flux densities [8]. The additional presence of large uncertainties of the heat flux density for a certain module/location requires dimensioning for the highest anticipated value (to exclude component failure), which results in over-cooling (too low outlet temperature, too high pumping power) when this highest anticipated value is not reached in operation. This is true for all cooling media, and calls for designing the plasma and the FW to reach a balanced surface power load distribution with a high quality of prediction. For a machine like DEMO, residual uncertainties have to be accepted in the design phase, and the priority of machine safety exceeds the objective of net electricity output.

In the view of the above cited anticipated heat flux densities, R&D for helium cooled first wall designs is ongoing: One set of concepts strives to provide solutions for up to about 1 MW/m^2 for the large parts of the FW surface. These solutions aim to be compatible with integrated as well as detached [9] FW concepts. Other concepts aim at very high heat fluxes (Objective: up to 5 MW/m^2) predicted for the hot spots, applicable mainly for detached FW concepts or limiters.

Apart from the thermal loads the FW channel walls are also loaded by the static pressure of the coolant. The internal pressure of the helium coolant is uniformly set to 8 MPa in all helium cooled concepts.

3. Optimization approaches

The optimization approach in this study is not specific to a certain blanket/FW design and thus does not adopt specific mechanical constraints from such designs. Quadratic (w = h) channels as shown in Fig. 1 are considered. The included loads are the thermal loads from the plasma (and with less magnitude from the breeder zone (BZ) side), which induce secondary stresses by temperature gradients, and the internal pressure loads from the cooling channels which induce primary membrane stresses as well as primary bending stresses.

According to [10] for an edge-held flat rectangular plate with thickness s_{pf} due to internal pressure load p the maximum bending stress is according to Eq. (1)

$$\sigma_{pb} = p \cdot \frac{\beta \cdot w^2}{s_{pf}^2} \quad \text{with } \beta = 0.5 \tag{1}$$

and the stress due to a temperature difference in a body is approximated by Eq. (2)

$$\sigma_{DT} = \Delta T \cdot \gamma \cdot E \cdot (1 - \nu) \tag{2}$$

where γ is the coefficient of linear thermal expansion, E is the Young Modulus, and ν (0.3 for steel) the Poisson ratio. The true magnitude of the temperature-induced stresses depends strongly on the applied mechanical constraints. For cases with thin dividing walls the temperature difference within a channel cross section can be estimated by

$$\Delta T = \dot{q}_{pf} \left(\frac{1}{h_{psc}} + \frac{s_{pf}}{\lambda_w} \right) \tag{3}$$

where $\dot{q}_{pf}$ is the incident heat flux density from the plasma, h_{psc} is the heat transfer coefficient on the plasma sided channel surface, and λ_w is the wall thermal conductivity. Thermal stresses are however not only caused by the heat flux through the plasma sided channel cover, but also by temperature differences over the complete component (see also Section 3.2).

Both stress components act in the same sense on the plasma side channel cover shell surfaces near the dividing walls where they add up to a maximum. The indicative Eqs. (1)–(3) explain that stress-optimization for a high heat flux FW implies a trade-off for the channel cover thickness s_{pf}. The optimum value of s_{pf} is a function of material properties and especially the requested wall heat flux density $\dot{q}_{pf}$: the higher $\dot{q}_{pf}$, the lower s_{pf} must be chosen.

The stress assessment for normal operation includes the criteria of Eqs. (4) and (5) [11] which are highlighted here because they were found to be the limiting ones in the designs studied for this paper.

$$\overline{P_L + P_b} \leq 1.5 \cdot S_m \left(\theta_m\right) \tag{4}$$

$$Max\left(\overline{P_L + P_b}\right) + \Delta Q \leq 3 \cdot S_m \left(\theta_m\right) \tag{5}$$

$P_L + P_b$ is the primary membrane- plus bending stress intensity, ΔQ the secondary stress range and $S_m\left(\theta_m\right)$ the material's allowable stress for the temperature θ_m averaged over the thickness of the shell. In order to conservatively limit creep issues, the condition $\theta_m < 500\,^{\circ}$C was also satisfied.

The followed optimization approach addresses the following elements:

- Heat-transfer-enhancement: Increasing material strength (yield $S_y\left(\theta_m\right)$ or creep rupture $S_r\left(\theta_m\right)$) by *globally decreasing* the material temperature.
- Heat-transfer-tuning: Locally adapt the heat transfer coefficients to *equalize* the component temperature field.
- Optimizing the shape of the load-carrying structural material around the channel to reduce stresses.

3.1. Heat transfer enhancement

In the follow-up of promising scoping studies [8,12], a number of heat transfer enhancing structure configurations has been investigated using scale resolving CFD methods [13,14]. The delayed Detached Eddy Simulation (DDES) approach for the transverse sharp-edged ribs (TER) was validated by dedicated experiments

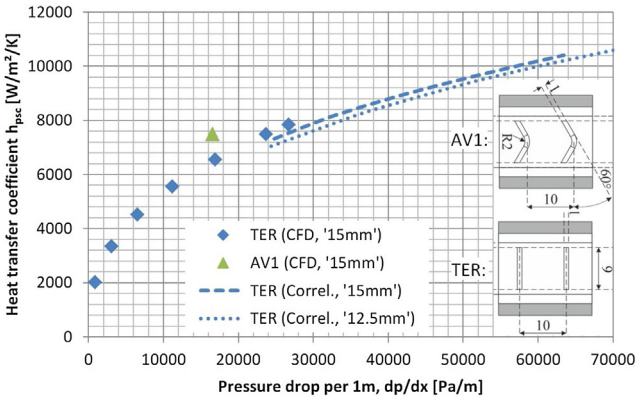

Fig. 2. Heat transfer coefficient (average value for plasma side channel surface) plotted versus the pressure drop per 1 m for several channel options at T = 350 °C, p = 8 MPa.

Table 1
Thermal-hydraulic design points for 1 MW/m².

Parameter	Case A	Case B1	Case B2	Case B3
$h = w\,[mm]$	15	12.5	12.5	12.5
s_{pf} [mm]	2.3	2.1	2.1	2.1
$\dot{m}\left[kg/s\right]$	0.1	0.06	0.07	0.08
h_{psc} [W/m²K]	10035	9475	10603	11689
$\theta_m\,[°C]$	491	493	482	473
$dp/dx\left[Pa/m\right]$	57546	51860	70164	91943
$P_{pump}/\dot{Q}_{th}$ [%]	4.4	2.8	4.5	6.7

(HETREX) and was applied to generate results in the Reynolds number range 25 000 – 160 000, resulting in correlations for Nusselt numbers and Fanning friction coefficients [15]. These results are the basis for this study. The sharp-edged V-shape ribs (AV1) were identified as even better performing geometry [14], offering an about 35% higher heat transfer at Reynolds number 105 000.

The averaged heat transfer coefficients on the plasma side channel wall h_{psc} are plotted vs. the pressure drop gradient dp/dx in Fig. 2.

Designs based on the TER rib, analysed thermal-hydraulically as outlined in [8], where θ_m is limited below 500 °C for $\dot{q}_{pf}$ = 1 MW/m², for helium (exit) temperature of 350 °C and pressure 8 MPa are listed in Table 1. Cases with w = 12.5 mm and w = 15 mm are chosen to reflect the up-to-date EU DEMO HCPB and the 2013 EU HCPB TBM designs. Case B1 offers the most economical pumping power of the studied cases.

3.2. Heat transfer tuning

In the previous section the outlet of the channel – where the highest helium temperature is effective – was studied. In a smooth channel, after the thermal run-in, an approximately linear wall temperature profile will evolve, following the gradual heat-up of the helium. With the objectives to smoothen the wall temperature profile (to reduce thermal induced stresses) and to economize rib-induced pressure drop and pumping power, the magnitude of the heat transfer enhancement can be adapted locally in such a way that the increase in the second summand of Eq. (6) is approximately balanced by the decrease of the third summand.

$$T_{psc}(x) = T_1 + \frac{\left(\dot{q}_{pf} + \dot{q}_b\right) \cdot x \cdot w_{pf}}{\dot{m} \cdot \overline{c_{p,fl}}} + \frac{\dot{q}_{pf}}{h_{psc}(x)} \tag{6}$$

This means that the heat transfer coefficient $h_{psc}(x)$ has to increase along the channel. In practice, this can be done by varying the rib height or/and switching the rib pattern (i.e. low profile transversal ribs near the channel entrance and high profile v-ribs near the exit).

Table 2
Thermal-mechnical results of FW with 1 MW/m².

Parameter	Case A	Case B1	Case B2	Case B3
$\overline{P_L + P_b}$ [MPa]	84	72	72	72
ΔQ [MPa]	316	321	311	300
θ_m [°C]	491	493	482	473
θ_{max} [°C]	540	535	525	518

3.3. Thermal-mechanical channel cross section optimization

Given the converse impact of s_{pf} on the pressure- and thermal-induced stresses respectively, this design parameter requires a careful balance. Since the bending stresses in the center axis of the channel cover wall are lower (and inversely oriented) than the ones along the corner-edge, it can be sought to adapt s_{pf} in spanwise direction. An example where the quarter-circle fillet of radius r_c = 2 mm was substituted by a biomimetically inspired "branch type" chamfer was investigated using a 3D FEM model. FEM simulations were performed with $\dot{q}_{pf} = 750\ kW/m^2$, $\dot{m} = 51\ g/s$, TER ribs with h_{psc} = 6100 W/m²/K, T_{He} = 347 °C. For the "branch-type" design, the wall thickness in the center was reduced (and the thickness in the fillets increased), until the stress peaks originating from pressure load occurring in the channel center and the fillet region were of similar magnitude. Less material is used in the branch type shapes. For this design two different thermal assumptions were investigated:

For the first case (BT1), the region of enhanced heat transfer on the plasma side was limited just to the extent of the ribs (9 mm width), conforming to the results for geometry TER. In this case a temperature hot spot emerges in the fillet region, which induces also an elevated secondary stress range.

For the second case (BT2), the region of enhanced heat transfer was extended over the full channel width (15 mm) including also the fillets. In this case, the temperature hot spot is reduced, and it showed that even the secondary stress range was slightly below the compared reference.

The investigated shapes and according results are illustrated in Fig. 3.

To make the strengthening of the channel chamfers successful, it is thus necessary to use ribs which enhance the heat transfer also in the corner-edges. This approach of optimization may prove especially useful if higher coolant pressures are envisaged.

The reference and BT2 case conform for the stress assessment criteria Eqs. (4) and (5) at 0.75 MW/m².

4. 1 MW/m² design points FEM analysis

Thermal-mechanical FEM analyses were performed using ANSYS 16.0 for the cases of Eurofer channels loaded with 1 MW/m² and 8 MPa presented in Section 3.1.: Case A with w = 15 mm and Cases B1/B2/B3 with w = 12.5 mm. Adiabatic conditions were applied to the lateral and axial surfaces for the thermal calculations. The heat transfer coefficient varied along the perimeter: Values for smooth channels [8] on the BZ side and the side walls, and increased heat transfer for TER ribs [15] on the straight part of the plasma sided channel. A linear interpolation between both values was applied along the chamfers. For the mechanical calculations a global curvature of the plate was inhibited by the coupled deformation conditions for the lateral wall surfaces, whereas axial elongation was allowed.

Results of all cases are shown in Table 2, exemplary temperature- and stress fields are plotted in Fig. 4. For all cases the

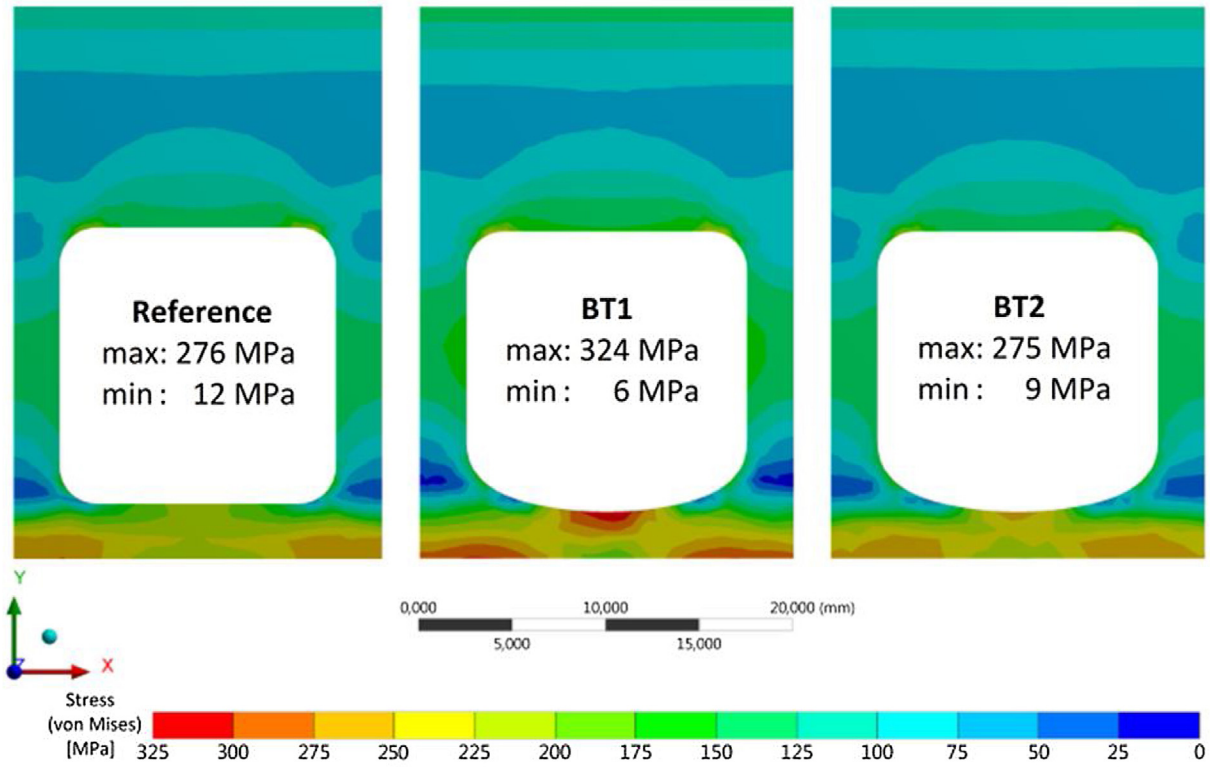

Case	$s_{pf,min}$	$\overline{P_L + P_b}$	ΔQ	θ_m
Reference	3.0 mm	58 MPa	288 MPa	511 °C
"BT1"	2.5 mm	53 MPa	325 MPa	556 °C
"BT2"	2.5 mm	52 MPa	286 MPa	512 °C

Fig. 3. Mises stress distribution in reference (left) and two biomimetically optimized (right) channel cross sections BT1 and BT2, with stress assessment indicators (below).

criteria of Eqs. (4) and (5) are met (Eurofer S_m (500 °C) = 145 MPa), the average shell temperature is below 500 °C, and the maximum temperature below 550 °C. In conjunction with Table 1 it is noted, that a design with margins can be more economically (judged by the pumping power) reached for w = 12.5mm than for w = 15mm. The stress fields of case A and B1 are differently patterned, because the wall thickness on the BZ side s_b = 12mm is the same (not scaled) for both cases, resulting in this part having a relatively higher stiffness in the B1 case, thus shifting the stress maximum to the plasma side. Further optimization potential is expected for thinning the side wall thickness ($w_{pf} - w$), reducing the chamfer radius r_c or shaping the plasma side wall (as shown in Section 3.3).

5. Fabrication procedures

The success of applying heat transfer enhancement structures is bound to the feasibility and economy of fabrication techniques.

In KIT, three different manufacturing routines for realization of blanket/FW components with internal cooling channels have been investigated. All three concepts are generally suitable for implementation of structures for heat transfer enhancement at the internal channel surfaces:

Concept i) is based on assembling two half-shells which are joined by HIP welding to create one solid part [16–18]. In this concept, the channel-internal surfaces are easily accessible during fabrication of the semi-finished shells, so the heat transfer enhancement structures can be conventionally machined on the surfaces with very moderate additional cost. This technique enables in principle all of the proposed heat transfer enhancement structures, but preferably those where the rib cross section has fillets can be machined with the least effort. The same procedure applies if the channels are fabricated by welding cover plates on a grooved base-plate.

The second option, concept ii) is to use Electrical Discharge Machining: Wire-cutting is used to fabricate the semi-finished channel (which is thus limited to any straight edged shape). To add the surface structures, two methods are possible:

a) The structures are formed by subsequent die-sink erosion [19]. With this technique, all of the proposed heat transfer enhancement structures can be created. Because the die-sink erosion costs scale with the sinking depth (or removed volume), a strong incentive to limit the structure heights exists.

b) Heat transfer enhancement is achieved by the "detached ribs", in which case the ribs can be implemented in a ladder-like structure which can be inserted into the channel in two lateral grooves (fixated by tack welds) which are machined in the same step as the wire-cutting of the channel. With this technique the additional costs are expected very low as the wire-cut costs scale by circum-

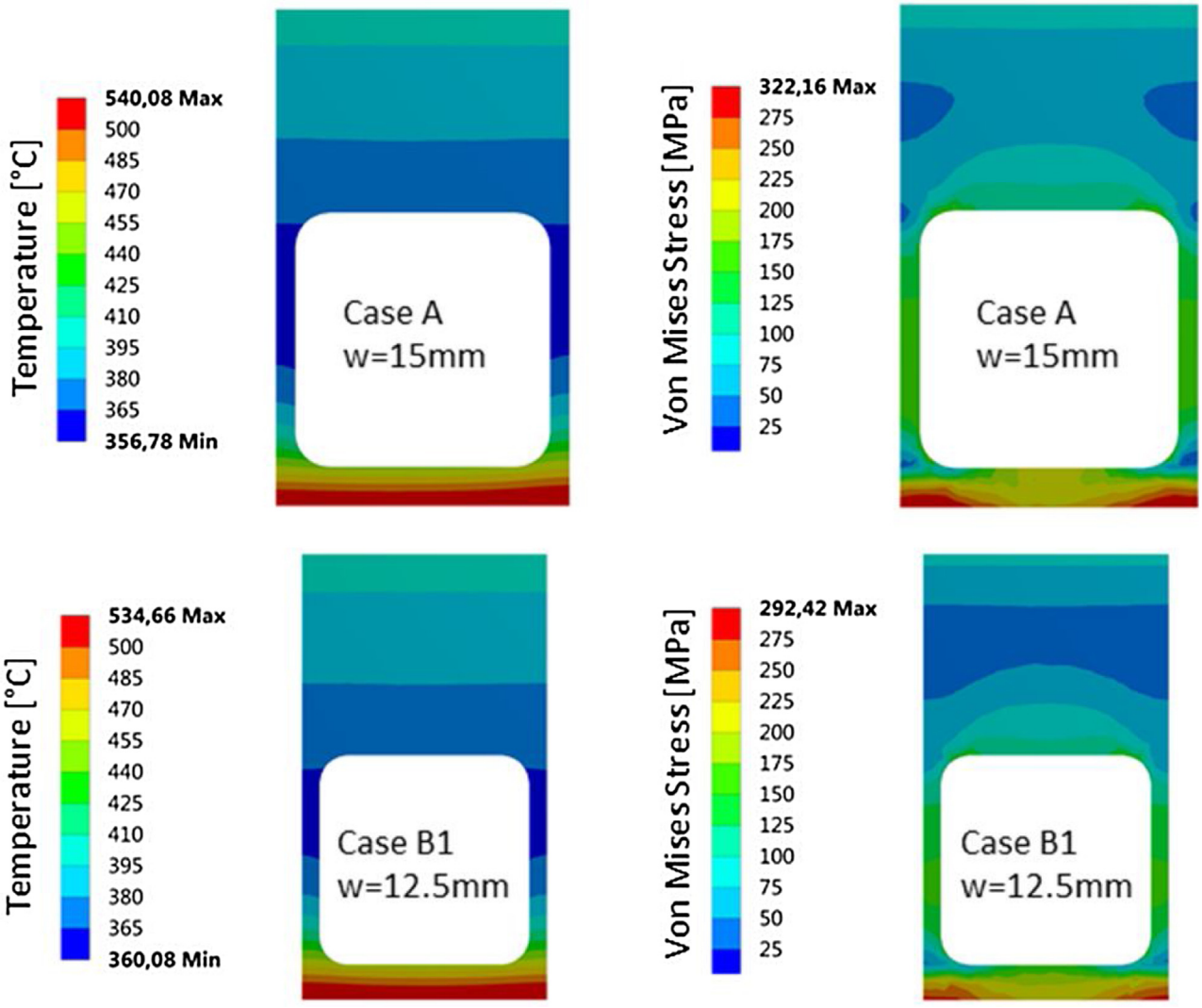

Fig. 4. Results from FEM: Temperature (left), stresses from 8 MPa pressure and from thermal loads combined (right).

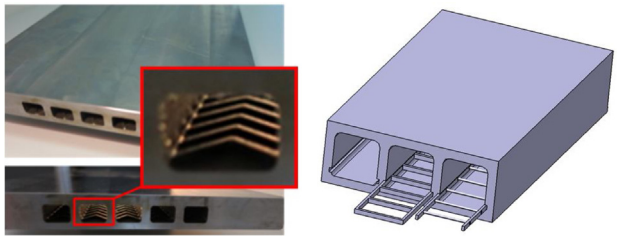

Fig. 5. Left: Fabrication test of a die-sink structured (v-ribs) FW channel plate. Right: CAD drawing of concept with detached ribs inserted as ladder-like structures.

ference (which is increased by <5%) and the ladder-like structures can be mass-produced, for example by punching or laser/water jet cutting from steel tape.

The channel fabrication concepts i) and ii) are technologically viable, and the conventional machining and die-sink fabrication of surface structures (see Fig. 5 left) are proven by prototypes. Their technological advantages and limitations (such as maximum plate size) are not significantly affected by the addition of surface structures. Both concepts can be combined to cold forming procedures in case that non-plane plates (e.g. 90° bends [19]) are required.

Even more flexibility in terms of channel flow paths and external geometry can be reached by concept iii) using generative/additive fabrication technologies (3D-manufacturing). This technology is under study in several labs and can be used for freely formed internal and external channel shapes. The application of Eurofer in Selective Laser Sintering manufacturing experiments has already been demonstrated successfully including a material characterization study, e.g. for a HCPB TBM Stiffening Plate. Heat transfer enhancement structures may be included inside the channels if needed without additional fabrication effort. However the external dimensions are currently limited to $\sim 0.3 \times 0.3 \times 0.3\,m^3$. The application of smart design solutions such as creation of hybrid components assembled e.g. by electron beam (EB) welding using aspects of concepts i) and ii) in combination with iii) result in a large range of options for realization of high heat flux gas cooled components [20].

6. Helium cooled FW for very high heat fluxes

Due to the present uncertainty in the local peak heat flux density definition for DEMO, solutions are also developed for loads in large excess of 1 MW/m^2. Currently, at KIT, the corresponding research is focused on solutions that are using the same materials as in the case of the breeding blanket: tungsten armor and Eurofer as structural material. The concepts exploit the possibilities (i) to increase the effective heat transfer area as well as (ii) to enhance the local heat

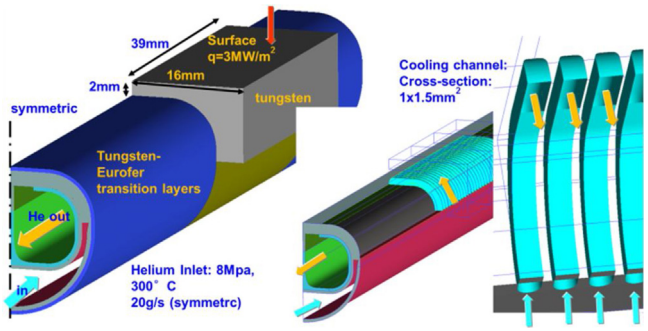

Fig. 6. Very high heat flux (multi-channel) cooling concept (only half of the cooling pipe is shown due to symmetry).

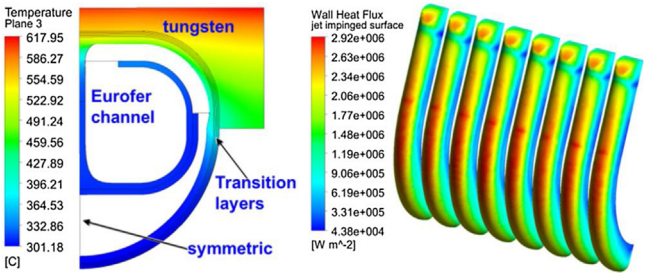

Fig. 7. Left: Temperature field on the cut-plane at middle of tungsten block. Right: wall heat flux on the channel wall surface at middle of tungsten block.

transfer coefficient. The currently most advanced concept from this family, based on parallel minichannels (multi-channel), is shown schematically in Fig. 6. This solution is using an annular distribution pipe with small channels (1 mm × 1.5 mm) embedded in the plasma facing side to increase the heat transfer area, combined with reduced thickness of the Eurofer wall of 0.5 mm. The outer pipe is used to distribute the helium to the small channels while the inner pipe is used as collector. The plasma facing side is covered with 2 mm thick tungsten armor. Between the tungsten and the structural material a transition layer of 0.5 mm is modeled. This transition layer is modeled as a combination of tungsten and Eurofer, the composition changing almost linearly from pure Eurofer at the surface of the pipe to pure tungsten at the armor side.

To evaluate the heat transfer performances, CFD simulations were done with Ansys-CFX V15 using the k-ω SST turbulence model. These simulations considered a helium flow rate of 20 g/s (for half-model as shown) with 8 MPa and 300 °C at the inlet. At the wall heat flux of 3 MW/m^2 the simulated maximum Eurofer temperature is 539 °C (<550 °C); the maximum tungsten temperature is 618 °C (see Fig. 7). The overall pressure loss is 0.88 bar with helium maximum velocity in the channels of 176 m/s. The averaged heat transfer coefficient based on helium inlet temperature is 23.4 kW/m^2/K on the multi-channel plasma-sided surface. The high mass flow rate per cooled surface area restricts such a solution to small fractions of the FW surface specifically prepared to handle high heat fluxes.

7. Summarizing conclusions and R&D outlook

With the currently available database on the thermal performance of FW-relevant heat transfer enhancement techniques, design points where the mean shell temperature is about 500 °C were found for a helium cooled first wall with a thermal load of 1 MW/m^2. This goal was reached by applying transverse edged ribs (TER) on the plasma side channel surface, and by adjusting the plasma sided cover wall thickness to 2.1–2.3 mm. The required helium mass flow rate and pressure drop lead to a tolerable pumping power in the range of 3–5% of the collected thermal power. The design study was completed with mechanical analyses which show acceptable stress levels. Even better performance is expected for the application of the V-shaped ribs, for which validation and analysis work is in progress. A focus will also be put on local tuning of the heat transfer coefficient, i.e. to augment the heat transfer in the chamfers and to increase it with flow length.

Parallel studies have assessed the fabrication feasibility of the proposed heat transfer enhancement structures for several of the existing blanket/FW fabrication strategies. The proposed structures are compatible with all of these strategies and in some cases can be produced with only moderate extra manufacturing effort.

Similar heat transfer enhancement techniques could be used for the cooling channels of the blanket stiffening plates as well, to reach higher outlet temperatures.

To further extend the sustainable heat flux density for helium cooled Eurofer first wall concepts, multi-channel concepts are under study, which up to now demonstrated sufficient cooling for heat loads up to 3 MW/m^2.

Acknowledgments

This work has been carried out within the framework of the EUROfusion Consortium and has received funding from the Euratom research and training programme 2014–2018 under the grant agreement 633053. The views and opinions expressed herein do not necessarily reflect those of the European Commission.

The authors would like to extend special thanks to Julien Aubert (CEA) Tom Barret (CCFE), Christian Bachmann and Ronald Wenninger (EUROfusion) for the fruitful discussions.

References

[1] L.V. Boccaccini, G. Aiello, J. Aubert, C. Bachmann, T. Barrett, A. Del Nevo, D. Demange, L. Forest, F. Hernandez, P. Norajitra, G. Porempovic, D. Rapisarda, P. Sardain, M. Utili, L. Vala, Objectives and status of EUROfusion DEMO blanket studies, Fus. Eng. Des. 109–111 (November (Part B)) (2016) 1199–1206.
[2] F. Cismondi, S. Kecskés, P. Pereslavtsev, E. Magnani, U. Fischer, Preliminary thermal design and related DEMO relevancy of the EU-HCPB TBM in vertical arrangement, Fus. Eng. Des. 85 (December) (2010) 2040–2044.
[3] G. Aiello, F. Gabriel, G. Rampal, J.-F. Salavy, A new cooling scheme for the HCLL TBM, Fus. Eng. Des. 84 (June (2–6)) (2009) 390–393.
[4] M. Ilić, G. Messemer, K. Zinn, R. Meyder, S. Kecskes, B. Kiss, Experimental and numerical investigations of heat transfer in the first wall of Helium-Cooled-Pebble-Bed Test Blanket Module—part 2: presentation of results, Fus. Eng. Des. 90 (January) (2015) 37–46.
[5] R. Wenninger, F. Arbeiter, J. Aubert, L. Aho-Mantila, R. Albanese, R. Ambrosino, C. Angioni, J.-F. Artaud, M. Bernert, E. Fable, A. Fasoli, G. Federici, J. Garcia, G. Giruzzi, F. Jenko, P. Maget, M. Mattei, F. Maviglia, E. Poli, G. Ramogida, C. Reux, M. Schneider, B. Sieglin, F. Villone, M. Wischmeier, H. Zohm, Advances in the physics basis for the European DEMO design, Nucl. Fusion 55 (2015).
[6] R. Wenninger, R. Kemp, F. Maviglia, H. Zohm, R. Albanese, R. Ambrosino, F. Arbeiter, J. Aubert, C. Bachmann, W. Biel, E. Fable, G. Federici, J. Garcia, A. Loarte, Y. Martin, T. Pütterich, C. Reux, B. Sieglin, P. Vincenzi, DEMO exhaust challenges beyond ITER, in: Proceedings of the 42nd EPS Conference on Plasma Physics, Lisbon, Portugal, 22nd–26th June, 2015 http://ocs.ciemat.es/EPS2015PAP/pdf/P4.110.pdf.
[7] R. Wenninger, et al., The DEMO wall load challenge, Nucl. Fusion 57 (Number) (2017).
[8] F. Arbeiter, C. Bachmann, Y. Chen, M. Ilić, F. Schwab, B. Sieglin, R. Wenninger, Thermal-hydraulics of helium cooled First Wall channels and scoping investigations on performance improvement by application of ribs and mixing devices, Fus. Eng. Des. 109–111 (November (Part B)) (2016) 1123–1129.
[9] T.R. Barrett, G. Ellwood, G. Pérez, M. Kovari, M. Fursdon, F. Domptail, S. Kirk, S.C. McIntosh, S. Roberts, S. Zheng, L.V. Boccaccini, J.-H. You, C. Bachmann, J. Reiser, M. Rieth, E. Visca, G. Mazzone, F. Arbeiter, P.K. Domalapally, Progress in the engineering design and assessment of the European DEMO first wall and divertor plasma facing components, Fus. Eng. Des. 109–111 (November (Part A)) (2016) 917–924.
[10] W.C. Young, R.G. Budynas, Roark's Formulas for Stress and Strain, seventh edition, McGraw Hill, 2002 (ISBN 0-07-072542-X).
[11] AFCEN, RCC-MRx–Design and Construction Rules for Mechanical Components of Nuclear Installations, 2012 edition, 2013 (1st addendum 2013, ISBN 2-913638-57-6).

[12] Yuming Chen, Frederik Arbeiter, Optimization of channel for helium cooled DEMO first wall by application of one-sided V-shape ribs, Fus. Eng. Des. 98–99 (2015) 1442–1447.
[13] S. Ruck, F. Arbeiter, Thermohydraulics of rib-roughened helium gas running cooling channels for first wall applications, Fus. Eng. Des. 109-111 (November (Part A)) (2016) 1035–1040.
[14] Sebastian Ruck, Benedikt Kaiser, Frederik Arbeiter, Thermal performance augmentation by rib-arrays for helium-gas cooled First Wall applications, Fusion Engineering and Design (2017), Available online 19 April, http://doi.org/10.1016/j.fusengdes.2017.03.171. (http://www.sciencedirect.com/science/article/pii/S0920379617303939) ISSN 0920-3796.
[14] Sebastian Ruck, Benedikt Kaiser, Frederik Arbeiter, Thermal performance augmentation by rib-arrays for helium-gas cooled First Wall applications, Fusion Engineering and Design (2017), Available online 19 April, http://dx.doi.org/10.1016/j.fusengdes.2017.03.171, (http://www.sciencedirect.com/science/article/pii/S0920379617303939) ISSN 0920-3796.
[15] S. Ruck, F. Arbeiter, Effects of rib-configuration on the thermal performance of one-sided heated, rib-roughened cooling channels, in: Proceed. 12th Int. Conf. on Heat Transfer, Fluid Mechanics and Thermodynamics, Malaga, Spain 2016, 2016.
[16] M. Rieth, B. Dafferner, S. Baumgärtner, S. Dichiser, T. Fabry, S. Fischer, W. Hildebrand, O. Palussek, H. Ritz, A. Sponda, R. Ziegler, H. Zimmermann, Cost effective fabrication of a fail-safe first wall, in: 1st Joint ITER-IAEA Technical Meeting on Analysis of ITER Materials and Technologies, Monaco, MC, 2010, November (23–25) https://publikationen.bibliothek.kit.edu/230081118.
[17] H. Neuberger, J. Rey, E. Materna-Morris, D. Bolich, T. Handl, T. Milker, Progress in the KIT approach for development of the HCPB TBM stiffening plate feasibility mock up fabrication, Fus. Eng. Des. 88 (June (5)) (2013) 265–270.
[18] A. Neuberger, J. von der Weth, Kit induced activities to support Fabrication, assembly and qualification of technology for the HCPB-TBM, Fus. Eng. Des. 86 (October (9–11)) (2011) 2039–2042.
[19] H. Neuberger, J. Rey, A.v.d. Weth, F. Hernandez, T. Martin, M. Zmitko, A. Felde, R. Niewöhner, F. Krüger, Overview on ITER and DEMO blanket fabrication activities of the KIT INR and related frameworks, Fus. Eng. Des. 96–97 (October) (2015) 315–318.
[20] H. Neuberger, J. Rey, M. Hees, E. Materna-Morris, D. Bolich, J. Aktaa, A. Meier, S. Fischer, C. Schorle, U. Fuhrmann, R. Heger, I. Dlouhý, L. Stratil, B. Kloetzer, Laser Beam Melting as manufacturing process for the realization of complex nuclear fusion and high heat flux components, presented at TOFE- manuscript number FST16-274, in: Fusion Science and Technology (American Nuclear Society), 2016.